mathematics

MDPI

Article

Distributed Finite-Time Coverage Control of Multi-Quadrotor Systems with Switching Topology †

Hilton Tnunay [1,*], Kaouther Moussa [2,3], Ahmad Hably [4] and Nicolas Marchand [4]

[1] KU Leuven, Faculty of Engineering Technology, 9000 Ghent, Belgium
[2] UPHF, CNRS, UMR 8201 - LAMIH, F-59313 Valenciennes, France
[3] INSA Hauts-de-France, F-59313 Valenciennes, France
[4] Univ. Grenoble Alpes, CNRS, Grenoble INP, GIPSA-lab, 38000 Grenoble, France
* Correspondence: hilton.tnunay@kuleuven.be
† This paper is an extended version of our paper published in IECON 2022—48th Annual Conference of the IEEE Industrial Electronics Society, Brussels, Belgium, 17–20 October 2022; pp. 1–6.

Abstract: This paper studies the distributed coverage control problem of multi-quadcopter systems connected with fixed and switching network topologies to guarantee the finite-time convergence. The proposed method modifies the objective function originating from the locational optimization problem to accommodate the consensus constraint and solves the problem within a given time limit. The coverage problem is solved by sending angular-rate and thrust commands to the quadcopters. By exploiting the finite-time stability theory, we ensure that the rotation and translation controllers of the quadcopters are finite-time stable both in fixed and switching communication topologies, able to be implemented distributively, and able to collaboratively drive the quadcopters towards the desired position and velocity of the Voronoi centroid independent of their initial states. After carefully designing and analyzing the performance, numerical simulations using a Robot Operating System (ROS) and Gazebo simulator are presented to validate the effectiveness of the proposed control protocols.

Keywords: coverage control; finite-time stability; distributed control; quadcopter; multiagent systems; robotic sensor network

MSC: 93D15

Citation: Tnunay, H.; Moussa, K.; Hably, A.; Marchand, N. Distributed Finite-Time Coverage Control of Multi-Quadrotor Systems with Switching Topology. *Mathematics* **2023**, *11*, 2621. https://doi.org/10.3390/math11122621

Academic Editors: Paolo Mercorelli, Oleg Sergiyenko, Oleksandr Tsymbal and Asier Ibeas

Received: 13 January 2023
Revised: 3 May 2023
Accepted: 29 May 2023
Published: 8 June 2023

1. Introduction

The robotics community has shown interest in the coverage control problem of robotic sensor networks (RSNs). There have been real-world issues motivating the rising attention to this problem, such as agriculture, search and rescue, wireless communication, and nuclear decommissioning, where sensor placement with a prdefined number of sensor determines the quality of the measured data [1,2]. For example, in precision agriculture, different color distribution in an agricultural farm may correspond to water stress, fertilizer shortage, or disease [3,4]. In order to capture and analyze the temporal information of this issue, unmanned aerial vehicles (UAVs) can be equipped with relevant sensors and be deployed to the farm. From the optimization point-of-view, finding the optimal position of the UAVs and the sensors becomes one of the main tasks of an RSN in order to maximize the coverage of the deployed sensors.

The existing literature shows extensive work to address the coverage control problem. Locational optimization, having its roots in the field of operations research, has been suggested as a method for determining the optimal agent locations based on an interest function. Centroidal Voronoi tessellation has emerged as a widely recognized approach for addressing this problem, as referenced in [5–8]. By adopting the locational optimization problem, a simple proportional controller was initially developed [8,9]. This algorithm is

improved to tackle the time-varying density coverage on a group of nonholonomic mobile robots in [10]. Different approaches to coverage control have been explored in [11–15] to alleviate the constraints related to unlimited, isotropic, and homogeneous sensing ranges, as well as convex environments. Solving the optimal coverage control problem of multiple robots can offer improved coverage, energy efficiency, robustness, and scalability, among other benefits. Nonoptimal approaches may be simpler to implement and require fewer computational resources but may not achieve the same level of performance as the optimal approach. Adaptive coverage control to estimate the information density function has been studied in [16–18]. Regarding the communication topology, the result in [19] includes a dynamically routing communication algorithm while optimizing the coverage control problem. The coverage control problem on a circle with unknown terrain roughness and time-varying communication delays has been studied in [20]. The mobile sensors cooperatively estimate the roughness function and are driven to their optimal positions using proposed control laws under some delay constraints. A reinforcement learning approach has also been studied to tackle the area coverage problem of networked UAVs in [21]. However, the coverage algorithm of multiple quadcopters from the control system perspective that guarantees timely convergence in a finite time for both fixed and switching communication topology has not been investigated among the existing strategies.

In various applications, such as postdisaster evacuation and nuclear decommissioning, the importance of timeliness has grown to prevent deteriorating situations [2]. In control theory, timeliness refers to the settling or convergence time of an autonomous system starting from initial values and reaching the origin. The research presented in [22] introduced the concept of finite-time stability analysis in control systems by demonstrating the dependence of convergence time on initial states. This finite-time strategy was applied to achieve finite-time consensus among teams of agents with different dynamics in [23–25], and also used for spacecraft pose synchronization based on dual quaternions in [26]. However, these results are dependent on initial values, causing longer convergence times when agents are initially separated by a large distance. To address this issue, [27] proposed a finite-time consensus controller that ensures convergence within a specified settling time boundary regardless of the initial states. Subsequently, [28] extended this result to the consensus of multiagent systems with double-integrator dynamics. Additionally, this approach was applied to design a finite-time consensus controller for networked systems with time delays in [29].

In this article, a distributed coverage control algorithm for a sensor network consisting of multiple quadcopters is introduced. The algorithm ensures finite-time stability in both fixed and switching communication topologies. This study builds upon our previous research that focused on the finite-time stability of the coverage control problem using a fixed communication topology [30]. The contributions of this work are highlighted as follows. Firstly, it differs from existing approaches by simultaneously addressing the locational optimization and consensus problems. This approach focuses on maintaining the position, velocity, and formation shape of the agents' Voronoi centroids. Secondly, the study leverages finite-time stability theory to ensure timely attainment of desired positions, velocities (i.e., Voronoi centroids), and attitudes in switching communication networks. Thirdly, since quadcopters are used as agents, the algorithm accounts for their nonlinear dynamics, which involve coupled translational and rotational motions. The algorithm guarantees stability of both translational and rotational motions within a specified time limit.

The structure of this paper is organized as follows. Section 2 briefly reviews the concepts of graph theory, locational optimization, and quaternions. Section 3 states the main problem addressed in this paper. Following that, the main algorithms for achieving finite-time coverage control of the quadcopter flock are presented in Section 4. Finally, numerical simulations validating the proposed algorithm are provided in Section 5, followed by concluding remarks in Section 6.

2. Preliminaries

2.1. Graph Theory

A graph, denoted as $\mathcal{G}(\mathcal{V}, \mathcal{E})$, is a collection of n vertices $\mathcal{V} = \{v_1, v_2, \ldots, v_n\}$ connected by a set of edges $\mathcal{E} \subseteq \mathcal{V} \times \mathcal{V}$. If an edge $(v_i, v_j) \in \mathcal{E}$ exists, it means that vertex v_i can receive information from vertex v_j. When both (v_i, v_j) and (v_j, v_i) exist in $\mathcal{E}$, the graph is referred to as undirected. The neighbor of vertex v_i, denoted as $v_j \in N_i \subset \mathcal{V}$, with $v_j \neq v_i$, is defined as a vertex connected to v_i through the edge $(v_i, v_j) \in \mathcal{E}$.

2.2. Locational Optimization

Consider the deployment of n robots within a convex environment represented by the set $\mathcal{Q} \subset \mathbb{R}^d$. The positions of all robots are denoted by the set $\mathcal{P} = p_i{}_{i=1}^{n} \subset \mathcal{Q}$, where p_i denotes the position of robot i.

The sensing unreliability function, denoted as $g : \mathcal{Q} \times \mathcal{Q} \to \mathbb{R}_+ : (x, p_i) \mapsto g(x, p_i)$, provides quantitative information about the sensing performance of agent i at position p_i when sensing point $x \in \mathcal{Q}$. In our context, we assume the sensing unreliability function to possess the following properties: isotropy, increasing, and convexity. An isotropic function exhibits a value that is independent of its direction. Therefore, we can redefine the function $g(x, p_i)$ as a norm-based function $f : \mathbb{R} \to \mathbb{R}_+$, such that $g(x, p_i) = f(\|x - p_i\|)$, where $i \in 1, 2, \ldots, n$.

The density function, or information distribution function, denoted by $\phi : \mathcal{Q} \to \mathbb{R}_+ : x \mapsto \phi(x)$, represents the spatial distribution of information within the environment. This function quantifies the importance of measuring a specific quantity at a particular point x in the set $\mathcal{Q}$.

After providing the definitions of the sensing unreliability function and density function, we introduce the locational optimization problem. Generated by the sensor positions at time t, $\mathcal{P}$, we are able to use the Voronoi tessellation of $\mathcal{Q}$ given by

$$V_i(p_i) = \{x \in \mathcal{Q} : \|x - p_i\| \leq \|x - p_j\|, \forall p_j \in \mathcal{P}, j \neq i\}. \tag{1}$$

In the following discussion, we use V_i conveniently to refer to $V_i(p_i)$. With this Voronoi partitions, the objective function of the locational optimization is formulated as

$$H(\mathcal{P}) = \sum_{i=1}^{n} \int_{V_i} g(x, p_i)\phi(q)dx. \tag{2}$$

With the defined conditions of the sensing unreliability function and density functions, the following lemma states the convexity of the objective function of the locational optimization.

Lemma 1 (Sensing Unreliability Function [30])**.** *Assume that the sensing unreliability function is isotropic, increasing, and convex in $p_i \in \mathcal{P}$, for all $i \in \{1, 2, \ldots, n\}$. Then, for a positive density function, the cost function H in (2) is convex.*

In this work, we make use of the quadratic sensing unreliability function defined as $f(\|x - p_i\|) = \|x - p_i\|^2$. By employing this quadratic function, we can incorporate the concept related to rigid body motion. This includes considering the mass, moment of inertia, and centroid of the i-th Voronoi region, which can be expressed as

$$M_{V_i} = \int_{V_i} \phi(x)dx, \; \mathcal{I}_{V_i} = \int_{V_i} x\phi(x)dx, \text{ and } C_{V_i} = \frac{\mathcal{I}_{V_i}}{M_{V_i}}, \tag{3}$$

respectively. Therefore, applying the parallel-axis theorem of rigid-body motion [31] to the cost function (2) leads to an equivalent expression given by

$$\min_{p \in \mathcal{P}} H(p), \text{ with } H(p) = \sum_{i=1}^{n} \mathcal{I}_{V_i} + \sum_{i=1}^{n} M_{V_i} \|p_i - C_{V_i}\|^2, \tag{4}$$

where $p = [p_1^\top, \ldots, p_n^\top]^\top \in \mathbb{R}^{nd}$ denotes the vectorized positions of the robots. The coverage control problem can be regarded as the task of designing control inputs for robots to drive them towards optimal positions, aiming to minimize the objective function of the locational optimization.

2.3. Quaternion-Based Rotation

In order to prevent singularities associated with Euler angles, the rotational movements of a rigid body are parameterized using quaternions, represented by the set $\mathbb{H} = \{q \in \mathbb{R}^4 | q^\top q = 1\}$. A quaternion $q_1 \in \mathbb{H}$ can be utilized to express the rotation from frame $\mathcal{W}^b$ to frame $\mathcal{W}^a$. The element-wise expression of this quaternion is given by $q_1 = \begin{bmatrix} \eta_1 & \bar{q}_1^\top \end{bmatrix}^\top = \begin{bmatrix} \cos\frac{\vartheta_1}{2} & k_1^\top \sin\frac{\vartheta_1}{2} \end{bmatrix}^\top$, where ϑ_1 is the rotation angle around the unit vector k_1. The quaternion conjugate is denoted by a superscripted asterisk, that is, $q_1^* = [\eta_1 \ -\bar{q}_1^\top]^\top \in \mathbb{H}$. In this paper, the dot operator represents the quaternion multiplication of quaternions, for example,

$$q_3 = q_1 \cdot q_2, \text{ for } q_1, q_2 \in \mathbb{H}. \tag{5}$$

A function $T : \mathbb{H} \to \mathbb{R}^{4\times 4}$ is defined as

$$T(q_1) = \begin{bmatrix} \eta_1 & -\bar{q}_1^\top \\ \bar{q}_1 & \eta_1 I + S(\bar{q}_1) \end{bmatrix}, \tag{6}$$

where the cross-product between two vectors $v_1, v_2 \in \mathbb{R}^3$ is represented using a skew-symmetric matrix operator $S \in \mathbb{R}^{3\times 3}$ such that $v_1 \times v_2 = S(v_1)v_2$. Utilizing this function, expression (5) becomes

$$q_3 = T(q_1)q_2. \tag{7}$$

The angular velocity of frame $\mathcal{W}^a$ with respect to frame $\mathcal{W}^b$, as observed from frame $\mathcal{W}^b$, is defined as $\omega_1 \in \mathbb{R}^3$. The connection between the time derivative of quaternion q_1 and the angular velocity ω_1 is expressed by

$$\dot{q}_1 = \frac{1}{2} q_1 \cdot \begin{bmatrix} 0 \\ \omega_1 \end{bmatrix} = \frac{1}{2} T(q_1) \begin{bmatrix} 0 \\ \omega_1 \end{bmatrix} = \frac{1}{2} \bar{T}(q_1)\omega_1, \tag{8}$$

where $\bar{T} = [-\bar{q}_1 \ (\eta_1 I + S(\bar{q}_1))^\top]^\top$ because the first column of $T(q_1)$ vanishes.

A rotation matrix can be created using quaternions through the application of Rodrigues' formula. The rotation matrix representing a rotation from frame $\mathcal{W}^b$ to $\mathcal{W}^a$ can be formulated as

$$R_1 = I + 2\eta_1 S(\bar{q}_1) + 2S^2(\bar{q}_1). \tag{9}$$

3. Problem Formulation

Consider a robotic sensor network comprising n quadcopters deployed in a convex space $\mathcal{Q} \subseteq \mathbb{R}^d$, and their connection topology is represented by a connected undirected graph $\mathcal{G}_n = (\mathcal{V}_n, \mathcal{E}_n)$. In this study, we investigate two cases: static and switching communication topology. For the static topology, we generate an undirected connected graph among the agents before deployment. In the switching case, we employ Delaunay triangulation to generate the communication graph in each new step, as indicated by Equation (1). The corresponding Laplacian of these graphs is denoted by $\mathcal{L}_n \in \mathbb{R}^{n\times n}$.

The locational optimization with consensus performance index in the coverage control problem can be constructed from (2) into

$$\min_{p\in\mathcal{P}} \tilde{H}(p), \text{ with } \tilde{H}(p) = H(p) + \frac{1}{2}(p - C_V)^\top \hat{\mathcal{L}}_n (p - C_V), \tag{10}$$

where $\hat{\mathcal{L}}_n = \mathcal{L}_n \otimes I_d \in \mathbb{R}^{nd\times nd}$, $p = [p_1^\top, \ldots, p_n^\top]^\top \in \mathbb{R}^{nd}$ and $C_V = [C_{V_1}^\top, \ldots, C_{V_n}^\top]^\top \in \mathbb{R}^{nd}$.

Quadcopter $i \in \mathcal{V}_n$ within the network possesses position, velocity, attitude, and angular rate denoted by $p_i \in \mathcal{Q}$, $v_i \in \mathbb{R}^3$, $q_i^c \in \mathbb{H}$, and $\omega_i^c \in \mathbb{R}^3$, respectively. The coordinate frames are illustrated in Figure 1, where we adhere to the ENU coordinate convention. The motions of a quadcopter can be categorized into two components: translation and rotation. The translational motion is determined by the attitude and the total thrust of the propellers. In the inertial frame, the quadcopter's translational dynamics, normalized by its mass, are governed by

$$\ddot{p}_i = q_i^c \cdot \bar{f}_i \cdot q_i^{c*} - \bar{g} = R_i^c \bar{f}_i - \bar{g}, \tag{11}$$

where $q_i^c \in \mathbb{S}^3$ is the unit quaternion denoting the current attitude of the quadcopter, $\bar{g} = [0\ 0\ g]^\top$ is the gravitational vector, with g being the gravitational acceleration, and $\bar{f}_i = [0\ 0\ f_i]^\top$ is the thrust control input, with f_i being the total thrust input. Following (8), the rotational motion of the quadcopter is governed by

$$\dot{q}_i^c = \frac{1}{2} q_i^c \cdot \begin{bmatrix} 0 \\ u_i^\omega \end{bmatrix} = \frac{1}{2} \bar{T}(q_1) u_i^\omega, \tag{12}$$

where, in this paper, the control input for the rotational motion is the angular rate u_i^ω.

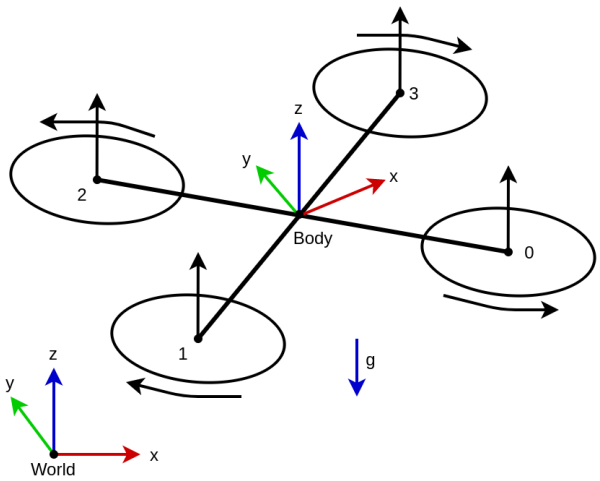

Figure 1. Coordinate frame of a quadcopter, adapted from our previous work in [30].

Using the transformed constrained optimization problem and the defined quadcopter dynamics in Equations (11) and (12), the objectives of this work are to design the quaternion-based attitude and distributed coverage controllers that guarantee convergence within a given settling time, regardless of the initial values, in both fixed and switching communication topologies.

4. Finite-Time Control Design

4.1. Translation Control with Fixed Topology

In the following control design, we tackle our first scenario: the coverage control problem with finite-time stability using a fixed communication topology. We introduce a distributed coverage controller that ensures the attainment of the optimal position and velocity within a finite duration, regardless of the initial positions, relying solely on information obtained from neighboring agents.

Let the performance index of the coverage problem be as defined in (10). The corresponding optimal point of this optimization is given by $p^\star = C_V - \frac{1}{2} M_V^{-1} \hat{\mathcal{L}}_n \tau_v$ for some vector $\tau_v \in \mathbb{R}^{nd}$. Given a fixed connected graph, it follows that the last term vanishes due to the zero eigenvalue of the Laplacian matrix $\hat{\mathcal{L}}_n$ such that $(p_1 - C_{V_1})^\star = \ldots = (p_n - C_{V_n})^\star$.

In other words, we can assert that the objective function $\tilde{H}(p)$ is at its optimum when the robots' positions converge to the optimal point $p^\star = C_V$ and consensus is reached. The velocity reaches its optimal value as $v^\star = \dot{C}_V$.

For all agent $i \in \mathcal{V}_n$, consider the following errors: $\tilde{\zeta}_i = [\tilde{p}_i^\top \ \tilde{v}_i^\top]^\top$ and $\tilde{\zeta}_{ij} = [\tilde{p}_{ij}^\top \ \tilde{v}_{ij}^\top]^\top$, where $\tilde{p}_i = p_i - C_{V_i}$, $\tilde{p}_{ij} = \text{sgn}(\tilde{p}_i - \tilde{p}_j)|\tilde{p}_i - \tilde{p}_j|$, $\tilde{v}_i = v_i - \dot{C}_{V_i}$, and $\tilde{v}_{ij} = \text{sgn}(\tilde{v}_i - \tilde{v}_j)|\tilde{v}_i - \tilde{v}_j|$. Since there are two terms to optimize in (10), by employing these errors, we design a controller consisting of centroid stabilizer and the consensus stabilizer. The controller responsible for driving the robots toward the centroids is proposed as

$$u_i^g = -\kappa_g \text{sgn}(\tilde{\zeta}_i)(|\tilde{\zeta}_i|^{\frac{m_\text{v}}{n_\text{v}}} + |\tilde{\zeta}_i|^{\frac{p_\text{v}}{q_\text{v}}}), \tag{13}$$

with $\kappa_g = [k_{gp} \ k_{gv}]^\top$, for $k_{gp}, k_{gv} > 0$, as well as some positive odd integers $m_\text{v}, n_\text{v}, p_\text{v}, q_\text{v}$, for $m_\text{v} > n_\text{v}$ and $p_\text{v} < q_\text{v}$. Similarly, with adjacency matrix $A = [a_{ij}]$, for $i \neq j$ and $i, j \in \mathcal{V}_n$, the consensus stabilizer to maintain the formation is given by

$$u_i^c = -\kappa_c \sum_{j=1}^{n} a_{ij} \text{sgn}(\tilde{\zeta}_{ij})(|\tilde{\zeta}_{ij}|^{\frac{m_\text{v}}{n_\text{v}}} + |\tilde{\zeta}_{ij}|^{\frac{p_\text{v}}{q_\text{v}}}), \tag{14}$$

with $\kappa_c = [k_{cp} \ k_{cv}]^\top$ and $k_{cp}, k_{cv} > 0$. Hence, the augmented controller reads

$$u_i^f = u_i^g + u_i^c + \bar{g}. \tag{15}$$

The following lemmas are useful for analyzing the performance of the designed control protocol.

Lemma 2 ([27]). *Let $x_1, x_2, \ldots, x_n \geq 0$. Then,*

$$\sum_{j=1}^{n} x_j^a \geq \left(\sum_{i=1}^{n} x_j \right)^a, \text{ for } a \in (0, 1).$$

Lemma 3 ([27]). *Let $x_1, x_2, \ldots, x_n \geq 0$. Then,*

$$\sum_{j=1}^{n} x_j^a \geq n^{1-a} \left(\sum_{i=1}^{n} x_j \right)^a, \text{ for } a > 1.$$

Lemma 4 ([27]). *The equilibrium point of the scalar system*

$$\dot{x} = -\alpha x^{\frac{a}{b}} - \beta x^{\frac{c}{d}}, \ x(0) = x_0,$$

where $\alpha, \beta > 0$, and a, b, c, d are positive odd integers satisfying $a > b$ and $c < d$, which are finite-time stable with the settling time given by

$$T < T_{\max} := \frac{1}{\alpha} \frac{b}{a-b} + \frac{1}{\beta} \frac{d}{d-c}.$$

Remark 1. *It is worth noticing that this lemma guarantees the finite-time convergence independent of the initial value of the system.*

In the subsequent theorem, we introduce our first result regarding the finite-time convergence of the suggested coverage control protocol for the fixed-topology situation, which is adapted from our conference paper [30].

Theorem 1 (Convergence of Finite-time Coverage Controller with Fixed Topology [30]). *Let a group of n agents be connected via a fixed undirected connected graph $\mathcal{G}_n = (\mathcal{V}_n, \mathcal{E}_n)$ with agent*

dynamics defined in (12) and (11). Let two adjacency matrices corresponding to this graph be denoted by $A_\alpha = [a_{ij}^{2n_\mathrm{v}/m_\mathrm{v}+n_\mathrm{v}}] \in \mathbb{R}^{n\times n}$ *and* $A_\beta = [a_{ij}^{2q_\mathrm{v}/p_\mathrm{v}+q_\mathrm{v}}] \in \mathbb{R}^{n\times n}$*, respectively, with* $m_\mathrm{v}, n_\mathrm{v}, p_\mathrm{v}, q_\mathrm{v}$ *being positive odd integers satisfying* $m_\mathrm{v} > n_\mathrm{v}$ *and* $p_\mathrm{v} < q_\mathrm{v}$*. Let the corresponding Laplacians* $\mathcal{L}_\alpha$ *and* $\mathcal{L}_\beta$ *have the smallest nonzero eigenvalues* λ_2^α *and* λ_2^β*, respectively. Then, there exist some constants* $\kappa_1, \kappa_2 > 0$ *such that the finite-time coverage problem can be solved by employing the coverage control protocol (15) with settling time expressed as*

$$T_f < T_{\max}^f := \frac{1}{\kappa_1}\frac{n_\mathrm{v}}{m_\mathrm{v}-n_\mathrm{v}} + \frac{1}{\kappa_2}\frac{q_\mathrm{v}}{q_\mathrm{v}-p_\mathrm{v}}. \tag{16}$$

Proof. Using the translational controller (15), the translational dynamics of the quadcopter can equivalently be expressed as

$$\dot{\tilde{\zeta}}_i = A\tilde{\zeta}_i + Bu_i^f = \begin{bmatrix} 0 & 1 \\ 0 & 0 \end{bmatrix}\tilde{\zeta}_i + \begin{bmatrix} 0 \\ 1 \end{bmatrix} u_i^f. \tag{17}$$

Define a Lyapunov function:

$$V^f(\tilde{\zeta}(t)) = \frac{1}{2}\sum_{i=1}^{n}\tilde{\zeta}_i^2(t). \tag{18}$$

With the system dynamics in (17), the time derivative of the candidate function is given by

$$\dot{V}^f(\tilde{\zeta}) = \dot{V}^g(\tilde{\zeta}) + \dot{V}^c(\tilde{\zeta}). \tag{19}$$

The centroid stabilizer in the first term of (19) can be expanded into

$$\dot{V}^g(\tilde{\zeta}) \leq -\lambda_{\min}^g \sum_{i=1}^{n}\tilde{\zeta}_i \mathrm{sgn}(\tilde{\zeta}_i)(|\tilde{\zeta}_i|^{\frac{m_\mathrm{v}}{n_\mathrm{v}}} + |\tilde{\zeta}_i|^{\frac{p_\mathrm{v}}{q_\mathrm{v}}}), \tag{20}$$

in which we already utilize the smallest eigenvalue of $A - B\kappa_g$ denoted by $\lambda_{\min}^g$. By using the fact that $|\tilde{\zeta}_i| = \tilde{\zeta}_i \mathrm{sgn}(\tilde{\zeta}_i)$, along with Lemmas (2) and (3), the centroid stabilizer term could be written as

$$\begin{aligned}\dot{V}^g(\tilde{\zeta}) &\leq -\lambda_{\min}^g\big(n^{\frac{n_\mathrm{v}-m_\mathrm{v}}{2n_\mathrm{v}}}\big(\sum_{i=1}^{n}\tilde{\zeta}_i^2\big)^{\frac{m_\mathrm{v}+n_\mathrm{v}}{2n_\mathrm{v}}} + n^{\frac{q_\mathrm{v}-p_\mathrm{v}}{2q_\mathrm{v}}}\big(\sum_{i=1}^{n}\tilde{\zeta}_i^2\big)^{\frac{p_\mathrm{v}+q_\mathrm{v}}{2q_\mathrm{v}}}\big) \\ &= -\lambda_{\min}^g\big(n^{\frac{n_\mathrm{v}-m_\mathrm{v}}{2n_\mathrm{v}}}(2V^f)^{\frac{m_\mathrm{v}+n_\mathrm{v}}{2n_\mathrm{v}}} + n^{\frac{q_\mathrm{v}-p_\mathrm{v}}{2q_\mathrm{v}}}(2V^f)^{\frac{p_\mathrm{v}+q_\mathrm{v}}{2q_\mathrm{v}}}\big).\end{aligned} \tag{21}$$

Similarly, the inequality of the consensus stabilizer from the second term of (19) can be expressed as

$$\dot{V}^c(\tilde{\zeta}) \leq -\lambda_{\min}^c \sum_{i=1}^{n}\tilde{\zeta}_i \sum_{j=1}^{n} a_{ij}\mathrm{sgn}(\tilde{\zeta}_{ij})(|\tilde{\zeta}_{ij}|^{\frac{m_\mathrm{v}}{n_\mathrm{v}}} + |\tilde{\zeta}_{ij}|^{\frac{p_\mathrm{v}}{q_\mathrm{v}}}), \tag{22}$$

where $\lambda_{\min}^c$ is the smallest eigenvalue of $A - B\kappa_c$. By utilizing the property of the adjacency matrix and also the fact that $|\tilde{\zeta}_{ij}| = \tilde{\zeta}_{ij}\mathrm{sgn}(\tilde{\zeta}_{ij})$, the consensus stabilizer term could be written as

$$\begin{aligned}\dot{V}^c(\tilde{\zeta}) &\leq -\frac{\lambda^c_{\min}}{2}\sum_{i=1}^{n}\sum_{j=1}^{n}a_{ij}((\tilde{\zeta}_{ij}^2)^{\frac{m_\mathrm{v}+n_\mathrm{v}}{2n_\mathrm{v}}}+(\tilde{\zeta}_{ij}^2)^{\frac{p_\mathrm{v}+q_\mathrm{v}}{2q_\mathrm{v}}})\\ &\quad+(a_{ij}^{\frac{2q_\mathrm{v}}{p_\mathrm{v}+q_\mathrm{v}}}\tilde{\zeta}_{ij}^2)^{\frac{p_\mathrm{v}+q_\mathrm{v}}{2q_\mathrm{v}}})\\ &\leq -\frac{\lambda^c_{\min}}{2}\big(n^{\frac{n_\mathrm{v}-m_\mathrm{v}}{2n_\mathrm{v}}}\big(\sum_{i=1}^{n}\sum_{j=1}^{n}a_{ij}^{\frac{2n_\mathrm{v}}{m_\mathrm{v}+n_\mathrm{v}}}\tilde{\zeta}_{ij}^2\big)^{\frac{m_\mathrm{v}+n_\mathrm{v}}{2n_\mathrm{v}}}\\ &\quad+n^{\frac{q_\mathrm{v}-p_\mathrm{v}}{2q_\mathrm{v}}}\big(\sum_{i=1}^{n}\sum_{j=1}^{n}a_{ij}^{\frac{2q_\mathrm{v}}{p_\mathrm{v}+q_\mathrm{v}}}\tilde{\zeta}_{ij}^2\big)^{\frac{p_\mathrm{v}+q_\mathrm{v}}{2q_\mathrm{v}}}\big)\end{aligned}\tag{23}$$

where the last inequality is obtained by employing Lemmas 2 and 3.

To analyze the graph, consider two adjacency matrices of connected undirected graphs $\mathcal{G}_\alpha$ and $\mathcal{G}_\beta$, denoted by $A_\alpha=[a_{ij}^{2n_\mathrm{v}/m_\mathrm{v}+n_\mathrm{v}}]\in\mathbb{R}^{n\times n}$ and $A_\beta=[a_{ij}^{2q_\mathrm{v}/p_\mathrm{v}+q_\mathrm{v}}]\in\mathbb{R}^{n\times n}$, respectively. The corresponding Laplacians are given by $\mathcal{L}_\alpha$ and $\mathcal{L}_\beta$. It follows that the inequality of the consensus stabilizer can equivalently be expressed as

$$\begin{aligned}\dot{V}^c(\tilde{\zeta}) &\leq -\frac{\lambda^c_{\min}}{2}(n^{\frac{n_\mathrm{v}-m_\mathrm{v}}{2n_\mathrm{v}}}(2\tilde{\zeta}^\top\mathcal{L}_\alpha\tilde{\zeta})^{\frac{m_\mathrm{v}+n_\mathrm{v}}{2n_\mathrm{v}}}\\ &\quad+n^{\frac{q_\mathrm{v}-p_\mathrm{v}}{2q_\mathrm{v}}}(2\tilde{\zeta}^\top\mathcal{L}_\beta\tilde{\zeta})^{\frac{p_\mathrm{v}+q_\mathrm{v}}{2q_\mathrm{v}}}),\end{aligned}\tag{24}$$

with $\tilde{\zeta}=[\tilde{\zeta}_1^\top,\ldots,\tilde{\zeta}_n^\top]^\top\in\mathbb{R}^{nd}$. Applying the Courant–Fischer theorem of the Laplacian matrices, $\tilde{\zeta}^\top\mathcal{L}_\alpha\tilde{\zeta}\geq\lambda_2^\alpha\|\tilde{\zeta}\|^2$ and $\tilde{\zeta}^\top\mathcal{L}_\beta\tilde{\zeta}\geq\lambda_2^\beta\|\tilde{\zeta}\|^2$ for $1_{nd}^\top\tilde{\zeta}=0_{nd}$, leads (24) to

$$\begin{aligned}\dot{V}^c(\tilde{\zeta}) &\leq -\frac{\lambda^c_{\min}}{2}(n^{\frac{n_\mathrm{v}-m_\mathrm{v}}{2n_\mathrm{v}}}(4\lambda_2^\alpha V^f)^{\frac{m_\mathrm{v}+n_\mathrm{v}}{2n_\mathrm{v}}}\\ &\quad+n^{\frac{q_\mathrm{v}-p_\mathrm{v}}{2q_\mathrm{v}}}(4\lambda_2^\beta V^f)^{\frac{p_\mathrm{v}+q_\mathrm{v}}{2q_\mathrm{v}}}).\end{aligned}\tag{25}$$

By adding (21) and (25), followed by some rearrangements, the time derivative of the Lyapunov function can be written as

$$\begin{aligned}\dot{V}^f(\tilde{\zeta}) &\leq -\frac{1}{2}n^{\frac{n_\mathrm{v}-m_\mathrm{v}}{2n_\mathrm{v}}}(2\lambda^g_{\min}+\lambda^c_{\min}(2\lambda_2^\alpha)^{\frac{m_\mathrm{v}+n_\mathrm{v}}{2n_\mathrm{v}}})(2V^f)^{\frac{m_\mathrm{v}+n_\mathrm{v}}{2n_\mathrm{v}}}\\ &\quad-\frac{1}{2}n^{\frac{q_\mathrm{v}-p_\mathrm{v}}{2q_\mathrm{v}}}(2\lambda^g_{\min}+\lambda^c_{\min}(2\lambda_2^\beta)^{\frac{p_\mathrm{v}+q_\mathrm{v}}{2q_\mathrm{v}}})(2V^f)^{\frac{p_\mathrm{v}+q_\mathrm{v}}{2q_\mathrm{v}}}.\end{aligned}\tag{26}$$

By denoting $\xi=\sqrt{2V^f}$ and $\dot{\xi}=2\dot{V}^f/\sqrt{2V^f}$ for $V^f(\tilde{\zeta})\neq 0$, we have

$$\begin{aligned}\dot{\xi} &\leq -\frac{1}{2}n^{\frac{n_\mathrm{v}-m_\mathrm{v}}{2n_\mathrm{v}}}(2\lambda^g_{\min}+\lambda^c_{\min}(2\lambda_2^\alpha)^{\frac{m_\mathrm{v}+n_\mathrm{v}}{2n_\mathrm{v}}})\xi^{\frac{m_\mathrm{v}+n_\mathrm{v}}{n_\mathrm{v}}}\\ &\quad-\frac{1}{2}n^{\frac{q_\mathrm{v}-p_\mathrm{v}}{2q_\mathrm{v}}}(2\lambda^g_{\min}+\lambda^c_{\min}(2\lambda_2^\beta)^{\frac{p_\mathrm{v}+q_\mathrm{v}}{2q_\mathrm{v}}})\xi^{\frac{p_\mathrm{v}+q_\mathrm{v}}{q_\mathrm{v}}}.\end{aligned}\tag{27}$$

Choosing positive odd integers $m_\mathrm{v}, n_\mathrm{v}, p_\mathrm{v}, q_\mathrm{v}$ satisfying $m_\mathrm{v}>n_\mathrm{v}$ and $p_\mathrm{v}<q_\mathrm{v}$ and employing Lemma 4 with the Comparison Principle [32] yields the boundary of the settling time, expressed as

$$T_f<T^f_{\max}:=\frac{1}{\kappa_1}\frac{n_\mathrm{v}}{m_\mathrm{v}-n_\mathrm{v}}+\frac{1}{\kappa_2}\frac{q_\mathrm{v}}{q_\mathrm{v}-p_\mathrm{v}},$$

with

$$\begin{aligned}\kappa_1&=\frac{1}{2}n^{\frac{n_\mathrm{v}-m_\mathrm{v}}{2n_\mathrm{v}}}(2\lambda^g_{\min}+\lambda^c_{\min}(2\lambda_2^\alpha)^{\frac{m_\mathrm{v}+n_\mathrm{v}}{2n_\mathrm{v}}}),\text{ and}\\ \kappa_2&=\frac{1}{2}n^{\frac{q_\mathrm{v}-p_\mathrm{v}}{2q_\mathrm{v}}}(2\lambda^g_{\min}+\lambda^c_{\min}(2\lambda_2^\beta)^{\frac{p_\mathrm{v}+q_\mathrm{v}}{2q_\mathrm{v}}}).\end{aligned}$$

It can be observed that the system is finite-time stable, i.e., $\lim_{t\to T^f_{\max}} V^f(\tilde{\zeta}) = 0$, implying that $\lim_{t\to T^f_{\max}} \|\tilde{\zeta}\| = 0$. □

In the the quadcopter model, we may obtain the thrust via $f_i = (u^f_i)^\top R^c_i [0\ 0\ 1]^\top$ utilizing the translational control input in (15).

4.2. Translation Control with Switching Topology

In this section, we address the second scenario examined in this research paper, which pertains to the finite-time coverage problem with a switching communication topology. The subsequent control design showcases a proposed controller that ensures the finite-time convergence of the robots' trajectory towards the optimal position and velocity, regardless of their initial positions, using only information from neighboring agents.

By employing similar performance index of the coverage problem defined in (10), this optimization problem has an optimal point given by $p^\star = C_V - \frac{1}{2} M_V^{-1} \hat{\mathcal{L}}_n \tau_v$ for some vector $\tau_v \in \mathbb{R}^{nd}$. As long as the time-varying undirected graph is connected, the last term vanishes due to the zero eigenvalue of the Laplacian matrix $\hat{\mathcal{L}}_n$ such that $(p_1 - C_{V_1})^\star = \ldots = (p_n - C_{V_n})^\star$. The objective function $\tilde{H}(p)$ is optimal when the position of the robots converge to the optimal point $p^\star = C_V$ and the consensus is achieved. The optimal value of the velocity is denoted by $v^\star = \dot{C}_V$.

In this switching topology scenario, the proposed centroid stabilizer, responsible for driving the robots toward the centroids, is formulated as

$$u^g_i = -\kappa_g \mathrm{sgn}(\tilde{\zeta}_i)(|\tilde{\zeta}_i|^{\frac{m_\mathrm{v}}{n_\mathrm{v}}} + |\tilde{\zeta}_i|^{\frac{p_\mathrm{v}}{q_\mathrm{v}}}), \tag{28}$$

with $\kappa_g = [k_{gp}\ k_{gv}]^\top$, for $k_{gp}, k_{gv} > 0$, as well as some positive odd integers $m_\mathrm{v}, n_\mathrm{v}, p_\mathrm{v}, q_\mathrm{v}$, for $m_\mathrm{v} > n_\mathrm{v}$ and $p_\mathrm{v} < q_\mathrm{v}$. Similarly, utilizing the adjacency matrix $A = [a_i j]$, for $i \neq j$ and $i, j \in \mathcal{V}_n$, the consensus stabilizer to maintain the formation is given by

$$u^c_i = -\kappa_c \sum_{j=1}^{n} a_{ij} \mathrm{sgn}(\tilde{\zeta}_{ij})(|\tilde{\zeta}_{ij}|^{\frac{m_\mathrm{v}}{n_\mathrm{v}}} + |\tilde{\zeta}_{ij}|^{\frac{p_\mathrm{v}}{q_\mathrm{v}}}), \tag{29}$$

with $\kappa_c = [k_{cp}\ k_{cv}]^\top$ and $k_{cp}, k_{cv} > 0$. Combining the centroid and consensus stabilizers, the augmented controller is

$$u^f_i = u^g_i + u^c_i + \bar{g}. \tag{30}$$

After formulating the controller, we present our second result for the finite-time convergence of the proposed coverage control protocol for the switching communication scenario extended from our previous result [30].

Theorem 2 (Convergence of Finite-time Coverage Controller with Switching Topology)**.** *Let a group of n agents have the agent dynamics defined in (12) and (11). Let these agents be connected via a switching connected Delaunay graph $\mathcal{G}_n(t) = (\mathcal{V}_n, \mathcal{E}_n(t))$ for all time $t > 0$. Let two adjacency matrices correspond to this graph, denoted by $A_\alpha = [a_{ij}^{2n_\mathrm{v}/m_\mathrm{v}+n_\mathrm{v}}] \in \mathbb{R}^{n\times n}$ and $A_\beta = [a_{ij}^{2q_\mathrm{v}/p_\mathrm{v}+q_\mathrm{v}}] \in \mathbb{R}^{n\times n}$, respectively, where $m_\mathrm{v}, n_\mathrm{v}, p_\mathrm{v}, q_\mathrm{v}$ are positive odd integers satisfying $m_\mathrm{v} > n_\mathrm{v}$ and $p_\mathrm{v} < q_\mathrm{v}$. Let the corresponding Laplacians $\mathcal{L}_\alpha$ and $\mathcal{L}_\beta$ for every time t have the smallest nonzero eigenvalues for all time $t > 0$ be $\lambda_2^{\alpha *} = \min_t \lambda_2^\alpha(\mathcal{L}_\alpha(\mathcal{G}_n))$ and $\lambda_2^{\beta *} = \min_t \lambda_2^\beta(\mathcal{L}_\beta(\mathcal{G}_n))$, respectively. Then, there exist some constants $\kappa_1, \kappa_2 > 0$ such that the finite-time coverage problem can be solved by employing the coverage control protocol (30) with settling time given by*

$$T_f < T^f_{\max} := \frac{1}{\kappa_1} \frac{n_\mathrm{v}}{m_\mathrm{v} - n_\mathrm{v}} + \frac{1}{\kappa_2} \frac{q_\mathrm{v}}{q_\mathrm{v} - p_\mathrm{v}}. \tag{31}$$

Proof. Using the translational controller (30), the translational dynamics of the quadcopter can equivalently be expressed as

$$\dot{\tilde{\zeta}}_i = A\tilde{\zeta}_i + Bu_i^f = \begin{bmatrix} 0 & 1 \\ 0 & 0 \end{bmatrix} \tilde{\zeta}_i + \begin{bmatrix} 0 \\ 1 \end{bmatrix} u_i^f. \tag{32}$$

Define a Lyapunov function:

$$V^f(\tilde{\zeta}(t)) = \frac{1}{2} \sum_{i=1}^{n} \tilde{\zeta}_i^2(t). \tag{33}$$

With the system dynamics in (32), the time derivative of the candidate function is given by

$$\dot{V}^f(\tilde{\zeta}) = \dot{V}^g(\tilde{\zeta}) + \dot{V}^c(\tilde{\zeta}). \tag{34}$$

The centroid stabilizer in the first term of (34) can be expanded into

$$\dot{V}^g(\tilde{\zeta}) \leq -\lambda_{\min}^g \sum_{i=1}^{n} \tilde{\zeta}_i \text{sgn}(\tilde{\zeta}_i)(|\tilde{\zeta}_i|^{\frac{m_V}{n_V}} + |\tilde{\zeta}_i|^{\frac{p_V}{q_V}}), \tag{35}$$

in which we already utilize the smallest eigenvalue of $A - B\kappa_g$ denoted by $\lambda_{\min}^g$. By using the fact that $|\tilde{\zeta}_i| = \tilde{\zeta}_i \text{sgn}(\tilde{\zeta}_i)$ along with Lemmas (2) and (3), the centroid stabilizer term could be written as

$$\begin{aligned} \dot{V}^g(\tilde{\zeta}) &\leq -\lambda_{\min}^g \big(n^{\frac{n_V - m_V}{2n_V}} \big(\sum_{i=1}^{n} \tilde{\zeta}_i^2 \big)^{\frac{m_V + n_V}{2n_V}} + n^{\frac{q_V - p_V}{2q_V}} \big(\sum_{i=1}^{n} \tilde{\zeta}_i^2 \big)^{\frac{p_V + q_V}{2q_V}} \big) \\ &= -\lambda_{\min}^g \big(n^{\frac{n_V - m_V}{2n_V}} (2V^f)^{\frac{m_V + n_V}{2n_V}} + n^{\frac{q_V - p_V}{2q_V}} (2V^f)^{\frac{p_V + q_V}{2q_V}} \big). \end{aligned} \tag{36}$$

Similarly, the inequality of the consensus stabilizer from the second term of (34) can be expressed as

$$\dot{V}^c(\tilde{\zeta}) \leq -\lambda_{\min}^c \sum_{i=1}^{n} \tilde{\zeta}_i \sum_{j=1}^{n} a_{ij} \text{sgn}(\tilde{\zeta}_{ij})(|\tilde{\zeta}_{ij}|^{\frac{m_V}{n_V}} + |\tilde{\zeta}_{ij}|^{\frac{p_V}{q_V}}), \tag{37}$$

where $\lambda_{\min}^c$ is the smallest eigenvalue of $A - B\kappa_c$. By utilizing the property of the adjacency matrix and also the fact that $|\tilde{\zeta}_{ij}| = \tilde{\zeta}_{ij} \text{sgn}(\tilde{\zeta}_{ij})$, the consensus stabilizer term could be written as

$$\begin{aligned} \dot{V}^c(\tilde{\zeta}) &\leq -\frac{\lambda_{\min}^c}{2} \sum_{i=1}^{n} \sum_{j=1}^{n} a_{ij} ((\tilde{\zeta}_{ij}^2)^{\frac{m_V + n_V}{2n_V}} + (\tilde{\zeta}_{ij}^2)^{\frac{p_V + q_V}{2q_V}}) \\ &\quad + (a_{ij}^{\frac{2q_V}{p_V + q_V}} \tilde{\zeta}_{ij}^2)^{\frac{p_V + q_V}{2q_V}}) \\ &\leq -\frac{\lambda_{\min}^c}{2} \big(n^{\frac{n_V - m_V}{2n_V}} \big(\sum_{i=1}^{n} \sum_{j=1}^{n} a_{ij}^{\frac{2n_V}{m_V + n_V}} \tilde{\zeta}_{ij}^2 \big)^{\frac{m_V + n_V}{2n_V}} \\ &\quad + n^{\frac{q_V - p_V}{2q_V}} \big(\sum_{i=1}^{n} \sum_{j=1}^{n} a_{ij}^{\frac{2q_V}{p_V + q_V}} \tilde{\zeta}_{ij}^2 \big)^{\frac{p_V + q_V}{2q_V}} \big) \end{aligned} \tag{38}$$

where the last inequality is obtained by employing Lemmas 2 and 3.

Using the relationship between Laplacian and adjacency matrices, it follows that the inequality of the consensus stabilizer can equivalently be expressed as

$$\dot{V}^c(\tilde{\zeta}) \leq -\frac{\lambda^c_{\min}}{2}(n^{\frac{n_\mathrm{v}-m_\mathrm{v}}{2n_\mathrm{v}}}(2\tilde{\zeta}^\top \mathcal{L}_\alpha \tilde{\zeta})^{\frac{m_\mathrm{v}+n_\mathrm{v}}{2n_\mathrm{v}}} + n^{\frac{q_\mathrm{v}-p_\mathrm{v}}{2q_\mathrm{v}}}(2\tilde{\zeta}^\top \mathcal{L}_\beta \tilde{\zeta})^{\frac{p_\mathrm{v}+q_\mathrm{v}}{2q_\mathrm{v}}}), \tag{39}$$

with $\tilde{\zeta} = [\tilde{\zeta}_1^\top, \ldots, \tilde{\zeta}_n^\top]^\top \in \mathbb{R}^{nd}$. Using the properties of the Laplacian matrices, $\tilde{\zeta}^\top \mathcal{L}_\alpha \tilde{\zeta} \geq \lambda_2^\alpha \|\tilde{\zeta}\|^2 \geq \lambda_2^{\alpha *}\|\tilde{\zeta}\|^2$ and $\tilde{\zeta}^\top \mathcal{L}_\beta \tilde{\zeta} \geq \lambda_2^\beta \|\tilde{\zeta}\|^2 \geq \lambda_2^{\beta *}\|\tilde{\zeta}\|^2$ for $1_{nd}^\top \tilde{\zeta} = 0_{nd}$, leads (39) to

$$\dot{V}^c(\tilde{\zeta}) \leq -\frac{\lambda^c_{\min}}{2}(n^{\frac{n_\mathrm{v}-m_\mathrm{v}}{2n_\mathrm{v}}}(4\lambda_2^{\alpha *}V^f)^{\frac{m_\mathrm{v}+n_\mathrm{v}}{2n_\mathrm{v}}} + n^{\frac{q_\mathrm{v}-p_\mathrm{v}}{2q_\mathrm{v}}}(4\lambda_2^{\beta *}V^f)^{\frac{p_\mathrm{v}+q_\mathrm{v}}{2q_\mathrm{v}}}). \tag{40}$$

By adding (36) and (40), followed by some rearrangements, the time derivative of the Lyapunov function can be written as

$$\begin{aligned}\dot{V}^f(\tilde{\zeta}) \leq &-\frac{1}{2}n^{\frac{n_\mathrm{v}-m_\mathrm{v}}{2n_\mathrm{v}}}(2\lambda^g_{\min} + \lambda^c_{\min}(2\lambda_2^{\alpha *})^{\frac{m_\mathrm{v}+n_\mathrm{v}}{2n_\mathrm{v}}})(2V^f)^{\frac{m_\mathrm{v}+n_\mathrm{v}}{2n_\mathrm{v}}} \\ &-\frac{1}{2}n^{\frac{q_\mathrm{v}-p_\mathrm{v}}{2q_\mathrm{v}}}(2\lambda^g_{\min} + \lambda^c_{\min}(2\lambda_2^{\beta *})^{\frac{p_\mathrm{v}+q_\mathrm{v}}{2q_\mathrm{v}}})(2V^f)^{\frac{p_\mathrm{v}+q_\mathrm{v}}{2q_\mathrm{v}}}.\end{aligned} \tag{41}$$

By denoting $\xi = \sqrt{2V^f}$ and $\dot{\xi} = 2\dot{V}^f/\sqrt{2V^f}$ for $V^f(\tilde{\zeta}) \neq 0$, we have

$$\begin{aligned}\dot{\xi} \leq &-\frac{1}{2}n^{\frac{n_\mathrm{v}-m_\mathrm{v}}{2n_\mathrm{v}}}(2\lambda^g_{\min} + \lambda^c_{\min}(2\lambda_2^{\alpha *})^{\frac{m_\mathrm{v}+n_\mathrm{v}}{2n_\mathrm{v}}})\xi^{\frac{m_\mathrm{v}+n_\mathrm{v}}{n_\mathrm{v}}} \\ &-\frac{1}{2}n^{\frac{q_\mathrm{v}-p_\mathrm{v}}{2q_\mathrm{v}}}(2\lambda^g_{\min} + \lambda^c_{\min}(2\lambda_2^{\beta *})^{\frac{p_\mathrm{v}+q_\mathrm{v}}{2q_\mathrm{v}}})\xi^{\frac{p_\mathrm{v}+q_\mathrm{v}}{q_\mathrm{v}}}.\end{aligned} \tag{42}$$

Choosing positive odd integers $m_\mathrm{v}, n_\mathrm{v}, p_\mathrm{v}, q_\mathrm{v}$ satisfying $m_\mathrm{v} > n_\mathrm{v}$ and $p_\mathrm{v} < q_\mathrm{v}$ and employing Lemma 4 with the Comparison Principle [32] yields the boundary of the settling time expressed as

$$T_f < T^f_{\max} := \frac{1}{\kappa_1}\frac{n_\mathrm{v}}{m_\mathrm{v}-n_\mathrm{v}} + \frac{1}{\kappa_2}\frac{q_\mathrm{v}}{q_\mathrm{v}-p_\mathrm{v}},$$

with

$$\begin{aligned}\kappa_1 &= \frac{1}{2}n^{\frac{n_\mathrm{v}-m_\mathrm{v}}{2n_\mathrm{v}}}(2\lambda^g_{\min} + \lambda^c_{\min}(2\lambda_2^{\alpha *})^{\frac{m_\mathrm{v}+n_\mathrm{v}}{2n_\mathrm{v}}}), \text{ and} \\ \kappa_2 &= \frac{1}{2}n^{\frac{q_\mathrm{v}-p_\mathrm{v}}{2q_\mathrm{v}}}(2\lambda^g_{\min} + \lambda^c_{\min}(2\lambda_2^{\beta *})^{\frac{p_\mathrm{v}+q_\mathrm{v}}{2q_\mathrm{v}}}).\end{aligned}$$

It can be observed that the system is finite-time stable, i.e., $\lim_{t\to T^f_{\max}} V^f(\tilde{\zeta}) = 0$, implying that $\lim_{t\to T^f_{\max}} \|\tilde{\zeta}\| = 0$. □

Similar to the the previous scenario, we may compute the thrust via $f_i = (u_i^f)^\top R_i^c [0\,0\,1]^\top$ by employing the translational control input in (30).

4.3. Rotation Control

Due to the interdependence of translational and rotational motion, it is necessary to develop an attitude controller that ensures finite-time stability.

Given the current and desired attitudes of the i-th quadcopter, denoted by $q_i^c = [\eta_i^c \;\; \bar{q}_i^{c\top}]^\top$ and $q_i^d = [\eta_i^d \;\; \bar{q}_i^{d\top}]^\top$, respectively, the error quaternion can be obtained via

$q_i^e = q_i^{c*} \cdot q_i^d = T(q_i^{c*}) q_i^d = [\eta_i^e \ \bar{q}_i^{e\top}]^\top$. For controller analysis, an error vector is also defined as follows:

$$e_{q_i^e} = \begin{bmatrix} 1 \mp \eta_i^e \\ \bar{q}_i^e \end{bmatrix}. \tag{43}$$

Differentiating this error yields the error dynamics expressed as

$$\dot{e}_{q_i^e} = \frac{1}{2} \bar{T}(q_i^e) u_i^\omega. \tag{44}$$

In this attitude control scheme, by employing the error vector, the angular-rate control command is defined as

$$u_i^\omega = -\kappa_\omega \mathrm{sgn}\left(\tilde{e}_{q_i^e}\right) \left(|\tilde{e}_{q_i^e}|^{\frac{m_\mathrm{w}}{n_\mathrm{w}}} + |\tilde{e}_{q_i^e}|^{\frac{p_\mathrm{w}}{q_\mathrm{w}}} \right) \tag{45}$$

with $\tilde{e}_{q_i^e} = [\bar{T}(q_i^e)]^\top e_{q_i^e}$ and $k_\omega > 0$.

The following theorem states our next result on the attitude controller of a quadcopter.

Theorem 3 (Convergence of Finite-time Rotational Controller)**.** *Let the attitude dynamics of a quadcopter be given by (12) and the error vector between the current and desired attitudes be given by (43). Then, given the control protocol (45), there exist some positive constants k_ω such that the equilibrium point of the error vector is finite-time stable with settling time given by*

$$T_a < T_{\max}^a := \frac{1}{\kappa_\omega} \left(\frac{n_\mathrm{w}}{m_\mathrm{w} - n_\mathrm{w}} + \frac{q_\mathrm{w}}{q_\mathrm{w} - p_\mathrm{w}} \right), \tag{46}$$

where $m_\mathrm{w}, n_\mathrm{w}, p_\mathrm{w}, q_\mathrm{w}$ are positive odd integers satisfying $m_\mathrm{w} > n_\mathrm{w}$ and $p_\mathrm{w} < q_\mathrm{w}$.

Proof. Define a Lyapunov function:

$$V^a(e_{q_i^e}) = \frac{1}{2} e_{q_i^e}^\top e_{q_i^e}. \tag{47}$$

Taking the derivative of the Lyapunov function yields

$$\dot{V}^a(e_{q_i^e}) = -\kappa_\omega \frac{1}{2} \tilde{e}_{q_i^e}^\top \mathrm{sgn}\left(\tilde{e}_{q_i^e}\right) \left(|\tilde{e}_{q_i^e}|^{\frac{m_\mathrm{w}}{n_\mathrm{w}}} + |\tilde{e}_{q_i^e}|^{\frac{p_\mathrm{w}}{q_\mathrm{w}}} \right), \tag{48}$$

where $\tilde{e}_{q_i^e} = [\bar{T}(q_i^e)]^\top e_{q_i^e}$, and the error dynamics with the proposed control command have been utilized. Since $\left|\tilde{e}_{q_i^e}\right| = \tilde{e}_{q_i^e} \mathrm{sgn}\left(\tilde{e}_{q_i^e}\right)$, (48) can be expressed as

$$\dot{V}^a(e_{q_i^e}) = -\kappa_\omega \frac{1}{2} \left(\left(\tilde{e}_{q_i^e}^2\right)^{\frac{m_\mathrm{w}+n_\mathrm{w}}{2n_\mathrm{w}}} + \left(\tilde{e}_{q_i^e}^2\right)^{\frac{p_\mathrm{w}+q_\mathrm{w}}{2q_\mathrm{w}}} \right) \tag{49}$$

Substituting $2V^a = \tilde{e}_{q_i^e}^2$ to (49) leads to

$$\dot{V}^a(e_{q_i^e}) = -\kappa_\omega \frac{1}{2} \left((2V^a)^{\frac{m_\mathrm{w}+n_\mathrm{w}}{2n_\mathrm{w}}} + (2V^a)^{\frac{p_\mathrm{w}+q_\mathrm{w}}{2q_\mathrm{w}}} \right). \tag{50}$$

By taking $\varrho = \sqrt{2V^a}$ and $\dot{\varrho} = 2\dot{V}^a / \sqrt{2V^a}$ for $V^a > 0$, (49) can equivalently be rewritten as

$$\dot{\varrho} = -\kappa_\omega \varrho^{\frac{m_\mathrm{w}}{n_\mathrm{w}}} - \kappa_\omega \varrho^{\frac{p_\mathrm{w}}{q_\mathrm{w}}}. \tag{51}$$

Therefore, utilizing the Comparison Principle [32] and Lemma 4 with some positive odd integers m_w, n_w, p_w, q_w, for $m_w > n_w$ and $p_w < q_w$, we may conclude that the settling time of the attitude system can be expressed as

$$T_a < T^a_{\max} := \frac{1}{\kappa_\omega}\left(\frac{n_w}{m_w - n_w} + \frac{q_w}{q_w - p_w}\right),$$

and the system is finite-time stable, i.e., $\lim_{t \to T^a_{\max}} V^a(e^e_{q_i}) = 0$, implying that $\lim_{t \to T^a_{\max}} \|e^e_{q_i}\| = 0$. □

Based on Equations (16) and (46), the computation of the boundary of the settling time of this coverage controller is indeed dependent on some controller parameters and the algebraic graph topology but independent of the initial values. Furthermore, the quadcopters will reach the optimal position and velocity within the settling time $T_{\text{sys}} = T^a + T^f < T^a_{\max} + T^f_{\max}$.

To obtain the desired quaternion, given translational control input (15) or (30) and desired heading ψ^d_i, let a heading vector $x^c_i = [\cos\psi^d_i \ \sin\psi^d_i \ 0]^\top$. Then, we may have a rotation matrix $R^d_i = [x^d_i \ y^d_i \ z^d_i]$ composed of $z^d_i = u^f_i / \|u^f_i\|$, $y^d_i = z^d_i \times x^c_i / \|z^d_i \times x^c_i\|$, and $x^d_i = y^d_i \times z^d_i / \|y^d_i \times z^d_i\|$. Accordingly, the desired quaternion can easily be obtained using a rotation matrix and quaternion relationship, such that $q^d_i = \text{rotmatToQuaternion}(R^d_i)$, as documented in [33].

5. Simulation Results

In this section, a series of numerical simulations are conducted to validate the proposed control protocols. The simulations are performed using the PX4 Autopilot software-in-the-loop (SITL) on the Gazebo simulator and the Mavros controller package integrated with the Robot Operating System (ROS) [34,35]. This simulation platform provides a highly realistic environment that closely emulates the behaviors and characteristics of real quadcopters equipped with the PX4 flight controller. The PX4 flight controller incorporates control input saturation in the low-level actuator controllers. The simulations are run on a computer with a Linux-based operating system, a 3.2-GHz processor, and 16-GB RAM. Figure 2 displays a screenshot of the simulator.

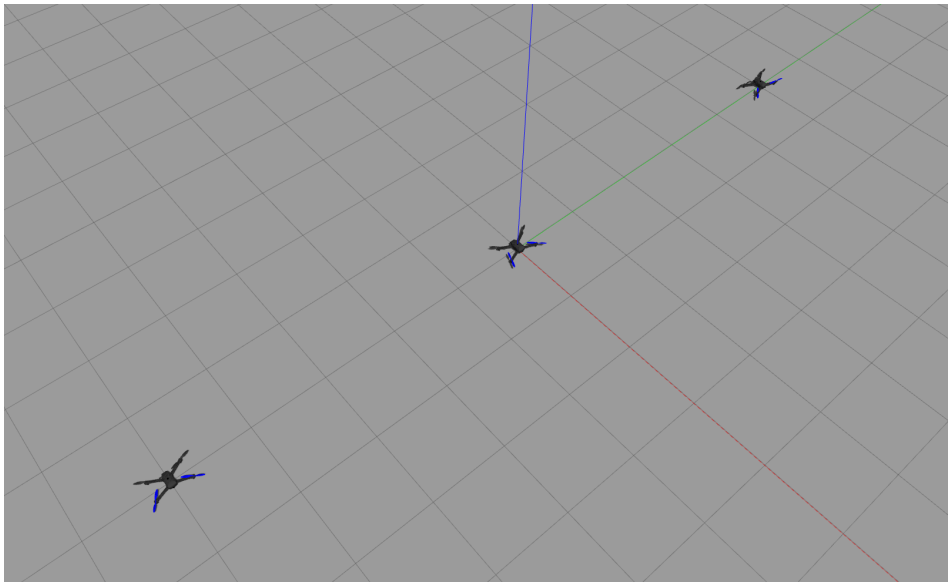

Figure 2. Quadcopters on Gazebo simulator, adapted from our previous work in [30].

Two scenarios are examined in this simulation: coverage control with fixed topology and coverage control with switching topology.

In the fixed topology scenario, nine quadcopters are randomly deployed within a bounded planar space defined by the coordinates (0,0), (0,1), (1,1), and (1,0). The quadcopters have constant altitude and adjust only their position and velocity in the $x-y$ plane. The distribution of information in this scenario is uniform. The controller parameters used are $m_{\mathrm{v}} = m_{\mathrm{w}} = 5$, $n_{\mathrm{v}} = n_{\mathrm{w}} = 3$, $p_{\mathrm{v}} = p_{\mathrm{w}} = 3$, $q_{\mathrm{v}} = q_{\mathrm{w}} = 5$, $\kappa_\omega = 0.8$, $\kappa_g = 0.5$, and $\kappa_c = 0.4$. The communication topology is represented by a complete graph among the nine agents, with the smallest nonzero eigenvalue being $\lambda_2 = 0.16$. Theoretical analysis (Theorems 1 and 3) suggests an estimated maximum settling time of $T_{\mathrm{sys}} = 23.850$.

Applying the control protocols described in Equations (15) and (45) to the quadcopter dynamics modeled by Equations (11) and (12), the resulting trajectories of the robots and the corresponding Voronoi partition are shown in Figure 3a. Additionally, Figure 3b displays the objective function, and Figure 3c illustrates the convergence trajectory of the error $\|p_i - C_{V_i}\|$. The control inputs of the agents are depicted in Figure 3d [30].

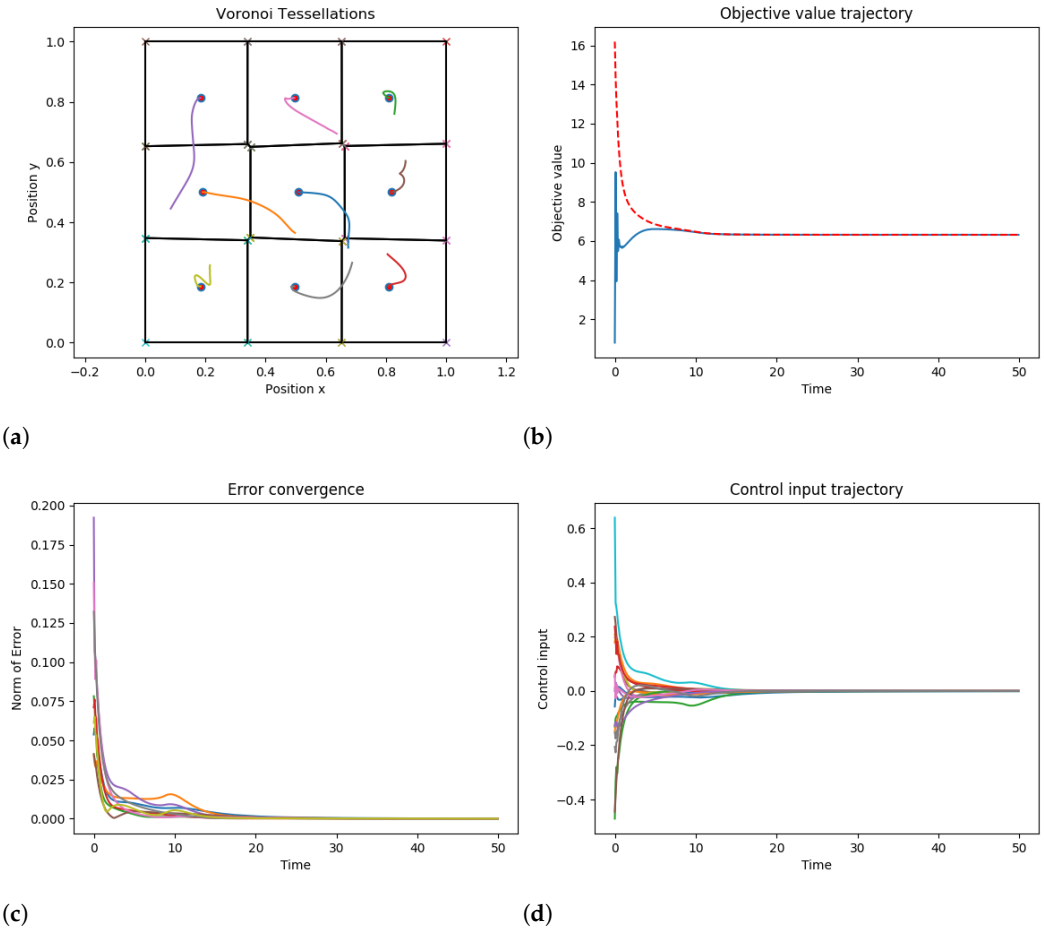

Figure 3. Finite-time coverage control simulation with fixed communication topology and uniform information distribution: (**a**) Trajectories and optimal Voronoi regions; (**b**) Objective function convergence, red-dashed line refers to the true objective function, blue line refers to the objective function computed by the agents in every iteration; (**c**) Trajectory errors; (**d**) Control inputs. Different colours in Subfigures (**a**), (**c**) and (**d**) refer to different trajectories of the quadcopters.

In the switching topology scenario, ten quadcopters are randomly deployed within a bounded planar space defined by the coordinates (0,0), (0,1), (1,1), and (1,0). Similar to the fixed topology case, the quadcopters have constant altitude and adjust only their position and velocity in the $x-y$ plane. However, the information distribution in this scenario exhibits two peaks. The controller parameters used are $m_{\mathrm{v}} = m_{\mathrm{w}} = 5$, $n_{\mathrm{v}} = n_{\mathrm{w}} = 3$, $p_{\mathrm{v}} = p_{\mathrm{w}} = 3$, $q_{\mathrm{v}} = q_{\mathrm{w}} = 5$, $\kappa_\omega = 0.8$, $\kappa_g = 0.5$, and $\kappa_c = 0.4$. The communication topology

is represented by a Delaunay graph among the ten agents, with the smallest nonzero eigenvalue being $\lambda_2 = 0.4615$. Theorems 2 and 3 suggest an estimated maximum settling time of $T_{\text{sys}} = 20.298$.

Applying the control protocols described in Equations (30) and (45) to the quadcopter dynamics modeled by Equations (11) and (12), the resulting trajectories of the robots and the corresponding Voronoi partition are shown in Figure 4a. Additionally, Figure 4b displays the objective function, and Figure 4c illustrates the convergence trajectory of the error $\|p_i - C_{V_i}\|$. The control inputs to drive the agents are plotted in Figure 4d.

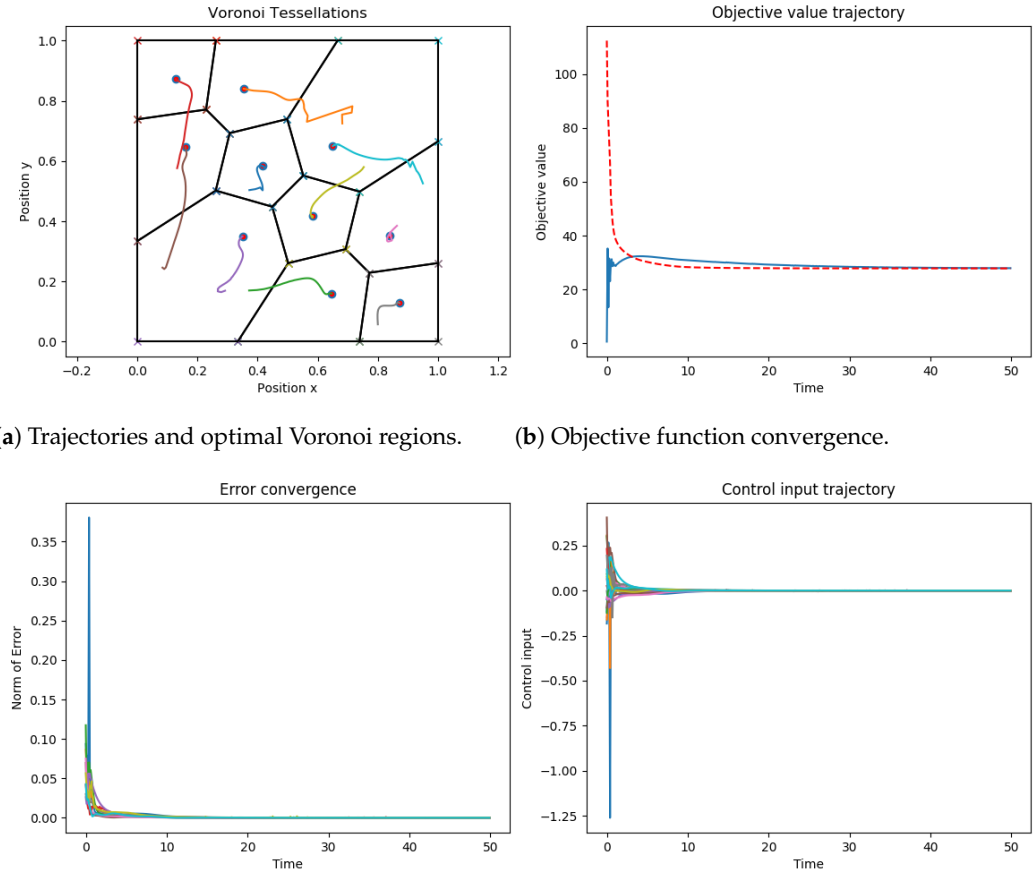

(**a**) Trajectories and optimal Voronoi regions.

(**b**) Objective function convergence.

(**c**) Trajectory errors.

(**d**) Control inputs.

Figure 4. Finite-time coverage control simulation with switching communication topology and diagonal-peak information distribution: (**a**) Trajectories and optimal Voronoi regions; (**b**) Objective function convergence, red-dashed line refers to the true objective function, blue line refers to the objective function computed by the agents in every iteration; (**c**) Trajectory errors; (**d**) Control inputs. Different colours in Subfigures (**a**), (**c**) and (**d**) refer to different trajectories of the quadcopters.

Figures 3 and 4 demonstrate the successful execution of the controllers, resulting in the alignment of the robots' positions with their respective centroids. In the first scenario, where the density function within the boundary is uniform, the distribution of robots per unit area appears similar. However, in the second scenario, quadcopters tend to cluster around the diagonal peaks. The error plots in Figures 3c and 4c confirm that the position error relative to the optimal position is minimized before the expected settling time $T_{\max}$. Additionally, Figures 3b and 4b illustrate the convergence of the objective function towards an optimal value once the centroids are reached.

Based on these results, it can be observed that the quadcopters, guided by the attractive coverage controller, move towards the optimal points from their initial positions. At certain

time instances $t = t_2$ (where $t_2 > 0$), some quadcopters exhibit higher convergence errors compared with earlier time $t = t_1$ (where $t_2 > t_1$). However, analyzing the objective function curves, it can be inferred that this behavior arises because, at time $t = t_2$, the algorithm has found a more efficient way to minimize the total objective function, i.e., moving a few quadcopters is easier than adjusting the others. These simulation results further validate that the protocols (15) and (30) successfully address the coverage control problem, enabling the quadcopters to converge close to the optimal positions within a finite time.

There remains the task of theoretically analyzing the proposed finite-time coverage control protocol under constrained control inputs to account for real quadcopter systems, where the control inputs may have bounds. This aspect will be investigated in future research, which will involve the utilization of actual quadcopters to validate the analysis.

6. Conclusions

In this paper, we studied the distributed coverage control problem of quadcopter sensor networks and ensured their finite-time stability both in fixed and switching communication topologies. The control protocols were classified into two schemes according to the motions: translation and rotation. By employing the reformulated locational optimization problem, a translational control protocol was developed to guide the quadcopters in tracking the position and velocity of the Voronoi centroid derived from the coverage control problem. Subsequently, the translational control command was fed into the rotational controller to determine the desired attitude of the quadcopter. Since the planar translation of the quadcopter was coupled with its attitude, we also proposed a rotational control protocol for each quadcopter based on quaternion to follow the desired attitude. The proposed translational and rotational protocols were carefully analyzed using the finite-time stability theory to ensure that the quadcopters' position and velocity converge to the Voronoi centroid position and velocity within a designed settling time, independent of the initial values, both in fixed and switching communication networks. Through simulations on the Gazebo simulator with ROS, we validated the performance of the proposed control protocols, where the centroids were reached within the expected duration. In future work, a number of experiments with real quadcopter systems with constrained control inputs will also be carried out at the GIPSA lab to verify the effectiveness of the algorithms.

Author Contributions: Conceptualization, H.T., K.M. and A.H.; Methodology, H.T., K.M. and A.H.; Validation, H.T. and K.M.; Formal analysis, H.T.; Investigation, K.M. and N.M.; Writing—original draft, H.T.; Writing—review & editing, H.T., K.M. and A.H.; Supervision, A.H. and N.M.; Project administration, N.M.; Funding acquisition, A.H. and N.M. All authors have read and agreed to the published version of the manuscript.

Funding: This research was supported by the TAMOS (TActical Multi-Objective Swarming UAVs) project.

Data Availability Statement: Data available with the corresponding author.

Conflicts of Interest: The authors declare no conflict of interest.

References

1. Carron, A.; Zeilinger, M.N. Model Predictive Coverage Control. *IFAC-PapersOnLine* **2020**, *53*, 6107–6112. [CrossRef]
2. Mei, Y.; Lu, Y.H.; Hu, Y.C.; Lee, C.S. Deployment strategy for mobile robots with energy and timing constraints. *Proc.-IEEE Int. Conf. Robot. Autom.* **2005**, *2005*, 2816–2821. [CrossRef]
3. Tsouros, D.C.; Bibi, S.; Sarigiannidis, P.G. A Review on UAV-Based Applications for Precision Agriculture. *Information* **2019**, *10*, 349. [CrossRef]
4. Zhang, J.; Tnunay, H.; Wang, C.; Lyu, X.; Ding, Z. Distributed Coverage Optimization and Control with Applications to Precision Agriculture. In Proceedings of the 2018 37th Chinese Control Conference (CCC), Wuhan, China, 25–27 July 2018; pp. 6836–6841. [CrossRef]
5. Okabe, A.; Suzuki, A. Locational optimization problems solved through Voronoi diagrams. *Eur. J. Oper. Res.* **1997**, *98*, 445–456. [CrossRef]
6. Okabe, A.; Boots, B.; Sugihara, K.; Chiu, S.N. *Spatial Tessellations: Concepts and Applications of Voronoi Diagrams*, 2nd ed.; Wiley Series in Probability and Statistics; Wiley: New York, NY, USA, 1995; Volume 26, p. 79. [CrossRef]

7. Pavone, M.; Arsie, A.; Frazzoli, E.; Bullo, F. Distributed Algorithms for Environment Partitioning in Mobile Robotic Networks. *IEEE Trans. Autom. Control* **2011**, *56*, 1834–1848. [CrossRef]
8. Cortes, J.; Martinez, S.; Karatas, T.; Bullo, F. Coverage Control for Mobile Sensing Networks. *IEEE Trans. Robot. Autom.* **2004**, *20*, 243–255. [CrossRef]
9. Salhi, S. Facility Location: A Survey of Applications and Methods. *J. Oper. Res. Soc.* **1996**, *47*, 1421–1422. [CrossRef]
10. Lee, S.G.; Diaz-Mercado, Y.; Egerstedt, M. Multirobot Control Using Time-Varying Density Functions. *IEEE Trans. Robot.* **2015**, *31*, 489–493. [CrossRef]
11. Cortés, J.; Martínez, S.; Bullo, F. Spatially-distributed coverage optimization and control with limited-range interactions. *ESAIM-Control. Optim. Calc. Var.* **2005**, *11*, 691–719. .:2005024. [CrossRef]
12. Pimenta, L.C.; Kumar, V.; Mesquita, R.C.; Pereira, G.A. Sensing and coverage for a network of heterogeneous robots. In Proceedings of the IEEE Conference on Decision and Control, Cancun, Mexico, 9–11 December 2008; pp. 3947–3952. [CrossRef]
13. Gusrialdi, A.; Hatanaka, T.; Fujita, M. Coverage control for mobile networks with limited-range anisotropic sensors. In Proceedings of the IEEE Conference on Decision and Control, Cancun, Mexico, 9–11 December 2008; pp. 4263–4268. [CrossRef]
14. Parapari, H.F.; Abdollahi, F.; Menhaj, M.B. Coverage control in non-convex environment considering unknown non-convex obstacles. In Proceedings of the 2014 2nd RSI/ISM International Conference on Robotics and Mechatronics, ICRoM 2014, Tehran, Iran, 15–17 October 2014; pp. 119–124. [CrossRef]
15. Kantaros, Y.; Thanou, M.; Tzes, A. Distributed coverage control for concave areas by a heterogeneous Robot-Swarm with visibility sensing constraints. *Automatica* **2015**, *53*, 195–207. [CrossRef]
16. Schwager, M.; Slotine, J.J.; Rus, D. Decentralized, adaptive control for coverage with networked robots. In Proceedings of the IEEE International Conference on Robotics and Automation, Rome, Italy, 10–14 April 2007; pp. 3289–3294. [CrossRef]
17. Martinez, S. Distributed interpolation schemes for field estimation by mobile sensor networks. *IEEE Trans. Control Syst. Technol.* **2010**, *18*, 491–500. [CrossRef]
18. Schwager, M.; Vitus, M.P.; Powers, S.; Rus, D.; Tomlin, C.J. Robust adaptive coverage control for robotic sensor networks. *IEEE Trans. Control Netw. Syst.* **2017**, *4*, 462–476. [CrossRef]
19. Kantaros, Y.; Zavlanos, M.M. Distributed communication-aware coverage control by mobile sensor networks. *Automatica* **2016**, *63*, 209–220. [CrossRef]
20. Wang, P.; Song, C.; Liu, L. Coverage Control for Mobile Sensor Networks with Unknown Terrain Roughness and Time-varying Delays. In Proceedings of the 2022 41st Chinese Control Conference (CCC), Hefei, China, 25–27 July 2022; pp. 1–6. [CrossRef]
21. Tamba, T.A. Optimizing the Area Coverage of Networked UAVs using Multi-Agent Reinforcement Learning. In Proceedings of the 2021 International Conference on Instrumentation, Control, and Automation (ICA), Bandung, Indonesia, 25–27 August 2021; pp. 197–201. [CrossRef]
22. Bhat, S.P.; Bernstein, D.S. Finite-time stability of continuous autonomous systems. *SIAM J. Control Optim.* **2000**, *38*, 751–766. [CrossRef]
23. Xiao, F.; Wang, L.; Chen, J.; Gao, Y. Finite-time formation control for multi-agent systems. *Automatica* **2009**, *45*, 2605–2611. [CrossRef]
24. Khoo, S.; Xie, L.; Man, Z. Robust finite-time consensus tracking algorithm for multirobot systems. *IEEE/ASME Trans. Mechatron.* **2009**, *14*, 219–228. [CrossRef]
25. Du, H.; Yang, C.; Jia, R. Finite-time formation control of multiple mobile robots. In Proceedings of the 6th Annual IEEE International Conference on Cyber Technology in Automation, Control and Intelligent Systems, IEEE-CYBER 2016, Chengdu, China, 19–22 June 2016; pp. 416–421. [CrossRef]
26. Wang, J.; Liang, H.; Sun, Z.; Zhang, S.; Liu, M. Finite-time control for spacecraft formation with dual-number-based description. *J. Guid. Control. Dyn.* **2012**, *35*, 950–962. [CrossRef]
27. Zuo, Z.; Tie, L. A new class of finite-time nonlinear consensus protocols for multi-agent systems. *Int. J. Control* **2014**, *87*, 363–370. [CrossRef]
28. Zuo, Z. Nonsingular fixed-time consensus tracking for second-order multi-agent networks. *Automatica* **2015**, *54*, 305–309. [CrossRef]
29. Wang, C.; Tnunay, H.; Zuo, Z.; Lennox, B.; Ding, Z. Fixed-Time Formation Control of Multirobot Systems: Design and Experiments. *IEEE Trans. Ind. Electron.* **2019**, *66*. [CrossRef]
30. Tnunay, H.; Moussa, K.; Hably, A.; Marchand, N. Distributed Finite-time Coverage Control of Multi-quadrotor Systems. In Proceedings of the IECON 2022—48th Annual Conference of the IEEE Industrial Electronics Society, Brussels, Belgium, 17–20 October 2022; pp. 1–6. [CrossRef]
31. Abdulghany, A.R. Generalization of parallel axis theorem for rotational inertia. *Am. J. Phys.* **2017**, *85*, 791–795. [CrossRef]
32. Khalil, H.K. *Nonlinear Systems*, 3rd ed.; Prentice-Hall: Upper Saddle River, NJ, USA, 2002.
33. Brescianini, D.; Hehn, M.; D'Andrea, R. *Nonlinear Quadrocopter Attitude Control*; Technical Report; ETH Zürich, Departement Maschinenbau und Verfahrenstechnik: Zürich, Swizerland, 2013; pp. 1–21. [CrossRef]

34. Meier, L.; Honegger, D.; Pollefeys, M. PX4: A node-based multithreaded open source robotics framework for deeply embedded platforms. In Proceedings of the 2015 IEEE International Conference on Robotics and Automation (ICRA), Seattle, WA, USA, 26–30 May 2015; pp. 6235–6240. [CrossRef]
35. Lim, J. Mavros_CONTROLLERS—Aggressive Trajectory Tracking Using Mavros for PX4 Enabled Vehicles. 2019. Available online: https://scholar.google.co.kr/citations?view_op=view_citation&hl=en&user=NOdnT3EAAAAJ&citation_for_view=NOdnT3EAAAAJ:zYLM7Y9cAGgC (accessed on 10 January 2023). [CrossRef]